Study of the output characteristics of nonlinear optical loop mirror on an erbium-doped mode-locked fiber laser*

ZHOU Fei (周飞), **ZHOU Xue-fang** (周雪芳)**, **BI Mei-hua** (毕美华), **YANG Guo-wei** (杨国伟), **HU Miao** (胡淼), **and LU Yang** (卢旸)

College of Communication Engineering, Hangzhou Dianzi University, Hangzhou 310018, China

(Received 17 May 2020; Revised 17 August 2020)

We experimentally discussed the output characteristics of a passively mode-locked erbium-doped fiber laser using a single-mode fiber (SMF) structure as a saturable absorber (SA) based on nonlinear optic loop mirror (NOLM). The NOLM acting as an SA has properties of controllable pulse interval and pulse width. Four different types of NOLMs are experimentally discussed and the results show that fine adjustment to the coupler ratio together with optimization of the SMF length inside the NOLM can simultaneously implement high pulse energy and pulse internal tunability. The laser configuration provides a method to generate well-performing mode-locked lasing, and the investigations of the effects of changing some parameters of the laser also provide some help for the development of mode-locked fiber laser based on NOLM.

Document code: A **Article ID:** 1673-1905(2021)05-0283-6

DOI https://doi.org/10.1007/s11801-021-0082-x

Nowadays, ultrafast fiber lasers have developed fast because of their many advantages of high robust performance, high optical quality and high efficiency[1-4]. They have varieties of applications in optical spectroscopy[5], precision metrology[6], optical sensing[7], biomedical instruments[8] and nonlinear optics[9]. Mode-locked fiber lasers have attracted great interest due to high quality ultrafast pulses generated in recent years[10]. In mode-locked fiber lasers, passively mode-locked fiber lasers with the advantages of compact and flexible geometry construction, low-cost and stable pulses output, have attracted tremendous attention.

The passive mode-locked fiber laser can be achieved either by artificial saturable absorber (SA) mechanisms such as nonlinear polarization rotation (NPR)[11] or by real SA devices such as carbon nanotubes (CNTs)[12], semiconductor saturable absorber mirrors (SESAMs)[13], antimonene[14] and graphene[15]. CNT is commercialized completely, but it can not achieve wide band saturable absorption. SESAM is the dominant scheme, which can provide saturable absorption with various performances. However, SESAM has a complex manufacturing technology. Graphene has many advantages, but the light absorption capacity is relatively low. SAs based on NPR are very sensitive to the slightest perturbation of the fiber cavity. Compared to these passively mode-locked techniques, the realization of nonlinear optic loop mirror (NOLM) is much simpler and no specific mode-locker is required. However, most of the previous research about the mode-locked fiber laser based on NOLM focuses only on the generation of lasing. And no experimental work has undertaken until now to investigate output characteristics of the coupler ratio and the length of single-mode fiber (SMF) in the NOLM.

Herein, to achieve the relation between the coupler ratio, the SMF length and the flattened output power of single-longitudinal mode (SLM) oscillation, we experimentally demonstrate a nanosecond rectangular pulse, passively mode-locked erbium-doped soliton fiber laser with simple structure based on NOLM. Here we present results obtained with four different types of NOLMs as SA. Our results show that fine adjustment to the coupler ratio together with optimization of the SMF length inside the NOLM can simultaneously implement high pulse energy and pulse internal tunability.

The schematic for the proposed mode-locked erbium-doped fiber (EDF) laser is depicted in Fig.1. All of the experimental devices are placed well and fixed with tape to avoid the disturbance from external environment. The experimental system is composed of a 980 nm pump laser (LD), a 980/1 550 nm wavelength division multiplexer (WDM), a 5-m-long EDF, an isolator (ISO), two

* This work has been supported in part by the Zhejiang Province Science and Technology Plan Projects (No.LGG19F050001), the National Natural Science Foundation of China (No.601705055), and the Zhejiang Provincial Natural Science Foundation of China (No.LY17F050012).

** E-mail: zhouxf@hdu.edu.cn

optical couplers (OCs), OC1 connected a segment of SMF (Corning, SMF-28) is used to form an NOLM, the NOLM acts as an SA, the SMF is deliberately inserted into the NOLM for exciting nonlinear effects to assist the self-mode-locking. The isolator is employed for ensuring the unidirectional propagation of the cavity. The output power is extracted from the cavity through the 20% exit port of OC2. An optical spectrum analyzer (OSA AQ6370B, Yokogawa Test & Measurement Corp.) is used to monitor the laser spectrum, and electric pulses are observed by Tektronix MDO3052, and frequency spectrum is observed by Rohde & Schwarz FPC1500 spectrum analyzer. The total cavity length without the external SMF-28 is about 8 m.

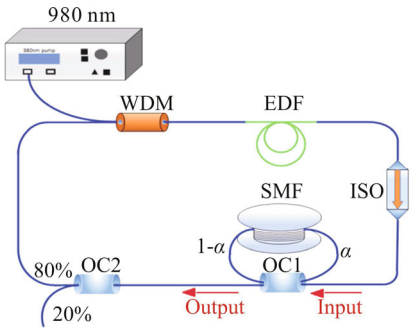

Fig.1 Schematic diagram of the proposed mode-locked fiber laser

The NOLM is employed to realize the passively mode-locked state in the proposed laser. The transmission characteristics of NOLM are analyzed below. The OC1 splits the input optical light according to the coupler ratio into two counter propagating waves, two beams of light travel for a circle along their direction, and then they recombine at the coupler. Assuming that the ratio of OC1 is α:1−α, the periodic transfer function[16] is

$$T=1-2\alpha(1-\alpha)\{1+\cos[(1-2\alpha)\gamma P_{\text{in}}L]\}, \quad (1)$$

where T, α, γ, P_{in} and L are the transmittance, coupler ratio (the port with SMF), nonlinear Kerr coefficient, input power and loop length, respectively. Eq.(1) shows that NOLM transmittance is decided by NOLM structure parameters, such as α and L. It is worth noting that an optimum length of the SMF and coupler ratio in the NOLM should be selected to attain the mode-locked lasing.

In order to get insight into the transmission peak profiles of the NOLM, different SMF lengths and coupler ratios inside the loop are experimentally researched. The result is shown in Fig.2, the horizontal axis is input power, whose unit is mW, and the vertical axis is the transmittance. Fig.2(a) shows the relation between the transmission and different SMF length. The modulation duration is labeled in Fig.2(a) with red lines. Label 1, 2 and 3 correspond to the three conditions of 300 m SMF, 600 m SMF and 10 km SMF. It can be seen that the SMF length has the important affection on the modulation duration, with the increase of SMF length, modulation duration will be decreased. As illustrated in Fig.2(b), modulation duration is labeled with red lines. Label 1, 2 and 3 correspond to the values of coupler ratio are 0.1, 0.3 and 0.4. Modulation depth can be easily seen from the difference value of the highest and lowest points. Different coupler ratio leads to different power of the first peak point, and results in different modulation duration and depth. The more balance the ratio is, the longer modulation period and deeper modulation depth are. These results provide theoretical guidance for the following experiments.

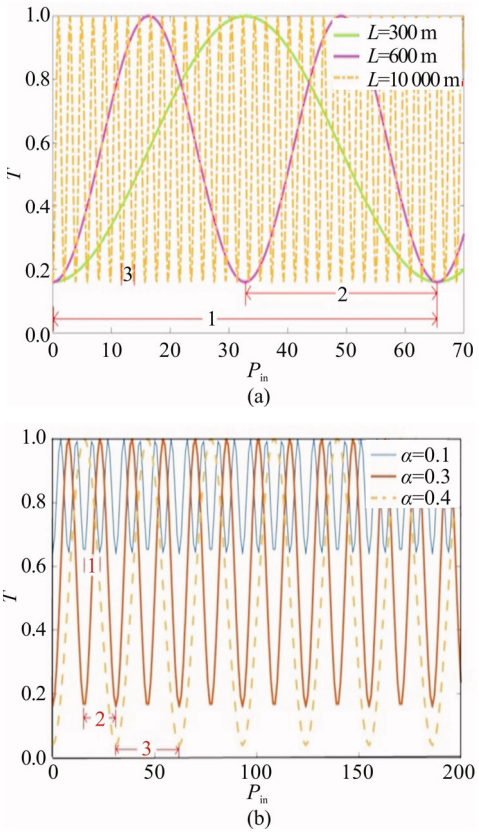

Fig.2 Effects of different (a) lengths of SMF and (b) coupler ratios on NOLM

In this experiment, different SMF lengths such as 300 m, 600 m and 10 km and different coupler ratios of OC1 such as 10:90 and 40:60 are selected to investigate the output characteristics. In every case, mode-locked operation is observed under certain suitable setting of EDF length and pump power.

When SMF is removed, the configuration can not realize mode-locked lasing output. When the length of SMF is 600 m, with the continuous improvement of pump power, the stability of the proposed laser is getting better. Firstly, we increase the pump power to a suitable value of 80 mW, stable mode-locked laser output spectrum can be achieved shown as Fig.3.

As illustrated in Fig.3(a), when pump power is 80 mW, the lasing central wavelength is 1 559.70 nm and the 3 dB bandwidth is 1.061 nm. It's apparently that the wavelength far from the central wavelength shows many joggles, which indicates that the laser is working in the

negative dispersion region[17]. These joggles are Kelly sidebands. The formation of Kelly sidebands is because of the periodic disturbance caused by weak dispersion and nonlinear effect. When Fig.3(b) shows the mode-locked pulse, the pulse separation is 5.1 μs, which gives a repetition rate of 208.05 kHz, which indicates that the oscillator is operating at the fundamental mode-locked state. The amplified single pulse is shown in Fig.3(c), the rough pulse width detected by oscilloscope is 56.03 ns, due to the limitation of the measuring instruments, the measured pulse width is bigger than expected, and Fig.3(d) shows the RF spectrum, it shows little frequency instability because optical fiber components are susceptible to external influences, and it's the same reason for Fig.3(c) shows a pulse shape distorted, the first RF peak is centered at 208.05 kHz, where the signal to noise ratio (*SNR*) is 56 dB, it's relatively competitive to other mode-lock lasers[18-21].

In order to further explore the output spectral of the proposed laser, we replace the SMF length with 300 m in the NOLM. The working threshold of this setting is 200 mW, which is lower than the first setting. The output spectrums are shown as Fig.4.

As shown in Fig.4(a), the spectrum shows apparent six order Kelly sidebands, it's the typical characteristic of working in negative dispersion region. Soliton pulses circulate through the laser cavity, if the influence of dispersion and nonlinearity in the resonator is weak, the pulse will experience some weak periodic disturbance due to dispersion and nonlinearity dispersion, which causes the soliton to propagate with a dispersion wave, and the relative phase of soliton and dispersive wave is changed constantly due to the nonlinear effect. However, there will be resonant coupling phenomenon happened in the cavity, leading to the phase between the dispersion wave and the optical soliton varies by integer multiples of 2 per cycle at certain frequencies. This effect shows some narrow peaks on soliton spectrum and is called Kelly sidebands[22]. However, Kelly sidebands phenomenon will not be found in mode-locked solid laser, because the intensity of dispersion and nonlinear effect in fiber laser cavity is much higher than that in solid laser cavity[23]. As shown in Fig.4(a), it can be seen that the central wavelength is 1 556.96 nm, and the 3 dB bandwidth is 3.50 nm. Compared to Fig.3(a), the Kelly sidebands become more apparent, because shorter length of SMF leads to weaker nonlinear effect, it will intensify the Kelly sidebands. Fig.4(b) displays the apparent mode-locked pulse spectrum, the pulse separation is 1.58 μs, and it shows slight wobble because of the interference of external environment.

In order to further discover the influences of the SMF length on the output characteristic of the laser, we replaced the SMF length with 10 km based on the former simulation, and repeat this experiment. During the experiment, when the pump power is higher than 40 mW, the laser could work in mode-locking regime. The output spectrum is shown as Fig.5.

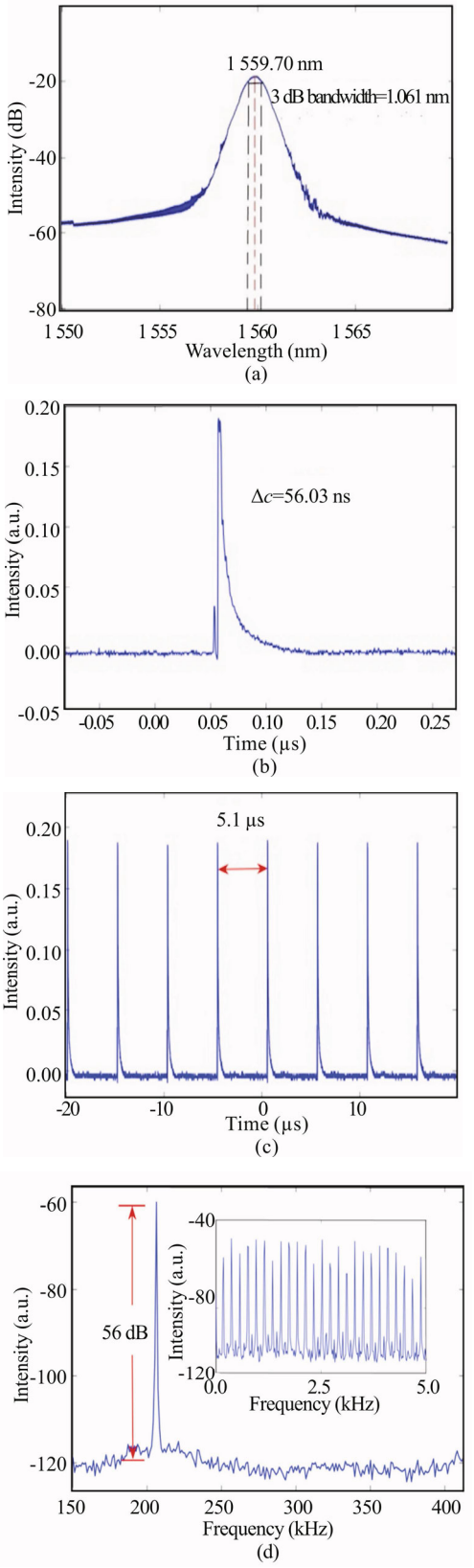

Fig.3 Single soliton operation at 80 mW when SMF is 600 m: (a) Optical spectrum; (b) Oscilloscope trace of the single pulse emission; (c) Single pulse after amplification; (d) RF spectrum at a fundamental frequency of 208.05 kHz (Inset is RF spectrum within 0—5 MHz.)

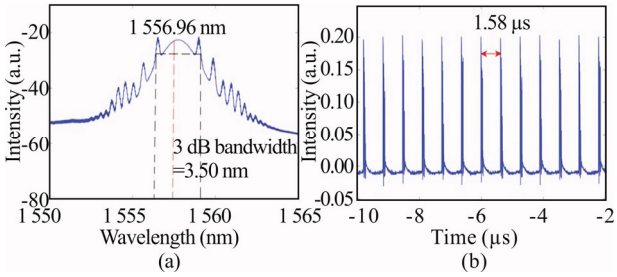

Fig.4 (a) Spectrum and (b) pulse at 200 mW when SMF is 300 m and coupler ratio is 90:10

Compared with the previous two value of SMF length, it is obviously that longer SMF in NOLM will leads to lower threshold pump power, because longer NOLM causes higher intensity of nonlinear effect and it needs lower pump power to achieve mode-locking. As illustrated in Fig.5(a), the central wavelength is 1 557.95 nm, which has little difference with the conditions of other length of SMF, and the 3 dB bandwidth of the spectrum is 2.29 nm. There is no Kelly sideband in the spectrum because the length of SMF is long enough to generate nonlinear effect. The apparent mode-locked pulse is depicted in Fig.5(b), the pulse interval and pulse intensity are 25.90 μs and 0.19, and the pulse bandwidth is 149.7 ns. The pulse period is matched with the cavity length.

Based on the former experiments, the longer the SMF is, the lower pump power is needed to get mode-locked lasing output. Otherwise, the coupler ratio is an important parameter of NOLM. We select a 40:60 OC1 in the NOLM to repeat the experiment under the condition that the length of SMF is 10 km, and the output results are shown in Fig.6.

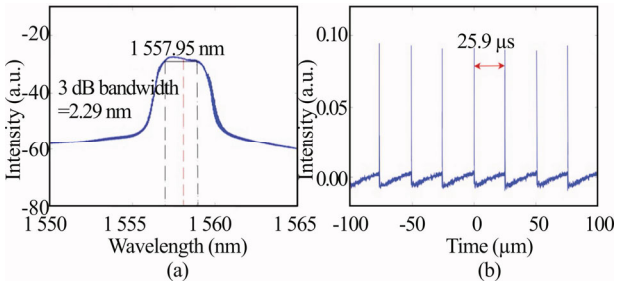

Fig.5 (a) Spectrum and (b) pulse at 40 mW pump power when SMF length is 10 km and coupler ratio is 90:10

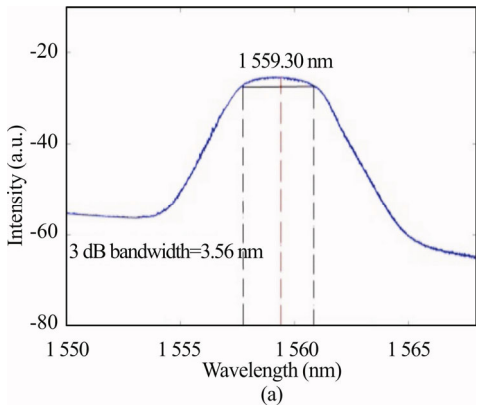

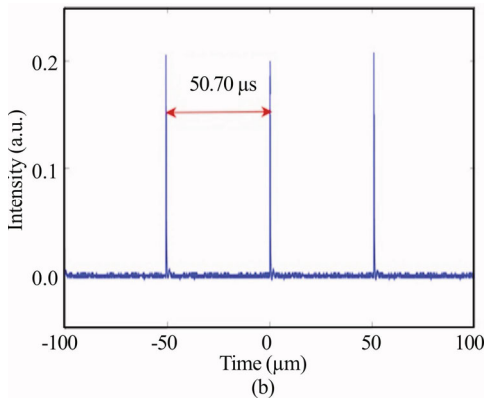

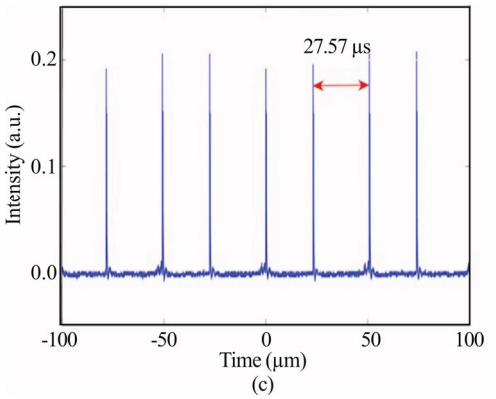

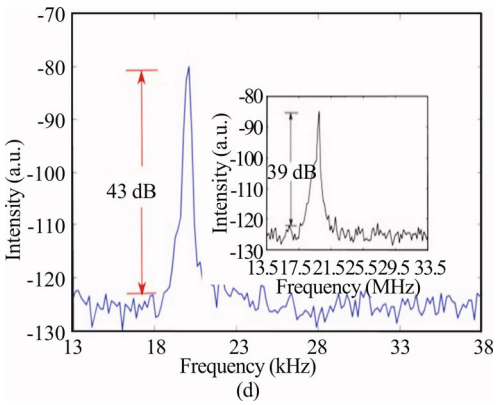

Fig.6 (a) Spectrum and (b) pulse at 30 mW pump power when coupler ratio is 40:60; (c) Pulse with 40 mW pump power; (d) RF spectrum with 40:60 coupler ratio (Inset is RF spectrum with 10:90 coupler ratio.)

By fine controlling the pump power, we can achieve the stable mode-locked lasing, when pump power is 30 mW, it will work in mode-locked regime, the threshold pump power is a little lower than the condition with the 10:90 coupler ratio. The central wavelength of the spectrum is 1 559.30 nm, and 3 dB bandwidth is 3.56 nm. Mode-locked pulse is shown in Fig.6(b), the pulse interval and width are 50.70 μs and 224 ns, respectively. In order to investigate the differences with the third setting, the pump power is fixed at 40 mW, the lasing output is shown in Fig.6(c), the pulse interval is 27.57 μs, and the width is 250.2 ns, compared to the third condition with 10:90 coupler ratio, the pulse interval varies little, while

the value of width becomes higher. Fig.6(d) shows the *SNR* whose horizontal axis is intensity and the vertical axis is frequency, the *SNR* is 43 dB when the coupler ratio is 40:60, and the inset shows the *SNR* with 10:90 coupler ratio is 39 dB.

To summarize the effects of different SMF lengths and different coupler ratios, we made two tables as follows.

As seen in Tab.1, the laser performance for different lengths of SMF with 10:90 coupler ratio, longer SMF causes stronger nonlinear effect, lower threshold pump power is needed, the optical spectrum difference caused by the SMF length is little and it can be neglected. With the length of SMF varying from 300 m to 10 km, the pulse period increases from 1.58 μs to 25.8 μs, and the pulse width increases from 21.16 ns to 149.7 ns. In terms of *SNR*, the condition of 300 m is the best, longer SMF will lead to lower *SNR*. Tab.2 shows the laser performance for different ratios of OC1 with 10 km SMF, the more balance the ratio is, the lower the threshold is. According to the above analysis, different parameters can be selected according to different needs and scenarios. And we can see from the two tables, central wavelength shows little change, because the experimental devices are fixed well and the model dispersion of SMF is low.

Tab.1 Laser performance for different lengths of SMF with ~10:90 coupler ratio

Length of NOLM	Performance parameters			
300 m	Mode-locking threshold (mW)	Central wavelength (nm)	3 dB bandwidth (nm)	Pulse period (μs)
	200	1 557.77	3.5	1.58
	Pulse width (ns)	Frequency (kHz)	*SNR* (dB)	
	21.46	630	57	
600 m	Mode-locking threshold (mW)	Central wavelength (nm)	3 dB bandwidth (nm)	Pulse period (μs)
	80	1 559.71	1.06	5.1
	Pulse width (ns)	Frequency (kHz)	*SNR* (dB)	
	56.03	208.05	56	
10 km	Mode-locking threshold (mW)	Central wavelength (nm)	3 dB bandwidth (nm)	Pulse period (μs)
	30	1 557.95	2.29	25.9
	Pulse width (ns)	Frequency (kHz)	*SNR* (dB)	
	149.7	20	39	

Tab.2 Laser performance for different ratios of OC1 with ~10 km SMF

Coupler ratio of OC1	Mode-locking threshold (mW)	Central wavelength (nm)	3 dB bandwidth (nm)	*SNR* (dB)
10:90	40	1 557.95	2.29	39
40:60	30	1 559.3	3.56	43

In order to further analyze the lasing characteristic of the proposed laser, we select the first setting to analyze the relation between the output spectrum of the laser and the pump power. Fig.7 shows the corresponding output spectra at different pump power. Fig.7(a) shows that different pump power influences the output power, *SNR* and the bandwidth of the spectrum, and obviously, the higher pump power leads to a little influence on the spectra. With the pump power increasing, the 3 dB bandwidth is also increased. When pump power is 100 mW, the 3 dB bandwidth is 2.32 nm, and while pump power is 600 mW, the 3 dB bandwidth is 2.99 nm, and the range of spectral bandwidth is about 0.67 nm. By varying the pump power from 100 mW to 600 mW, the *SNR* is increased from 17.63 dB to 19.97 dB.

The relation between the pulse and pump power is shown in Fig.7(b), and the pump powers are 300 mW, 400 mW, 500 mW, and 600 mW, respectively.

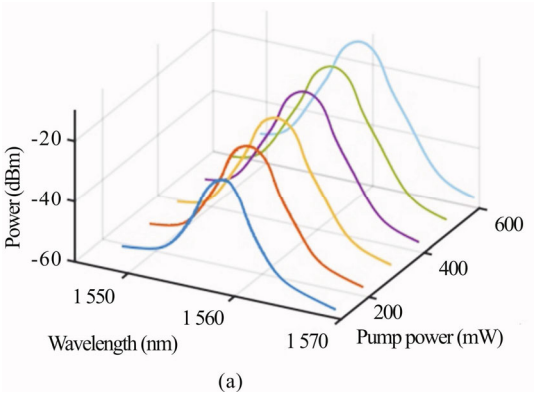

(a)

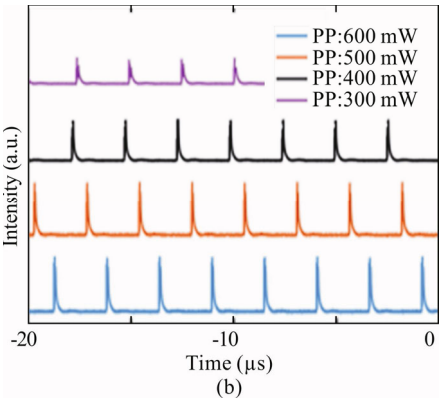

Fig.7 The output (a) spectra and (b) pulses at different pump power

There are four main observations from above mentioned results. First, the length of the SMF inside the NOLM plays a crucial role in the spectral shaping process of the laser. Second, the output pulse can be scaled up with proper SMF length and suitable coupler ratio. The longer the length of SMF is, the lower threshold pump power is needed, and bigger coupler ratio leads to the pulse spectrum smoother. The last one is the pulse energy arising from the input pump power. The minimum pulse width is 21.46 ns and its corresponding *SNR* is 57 dB. Moreover, the proposed laser features a simple configuration, stable operation and tunable pulse width, which may find applications in the field of optical metrology and interferometry, optical data storage and optical communications.

References

[1] M. E. Fermann and I. Hartl, Nat. Photon. **7**, 868 (2013).
[2] D. Deng, L. Zhan, Z. Gu, Y. Gu and Y. Xia, Opt. Express **17**, 4284 (2009).
[3] U. Keller, Nature **424**, 831 (2003).
[4] T. Feng, D. Ding, Z. Zhao, H. Su, F. Yan and X. Yao, Laser Phys. Lett. **13**, 105104 (2016).
[5] N. P. Barnes, B. M. Walsh, D. J. Reichle and R. J. De Young, Opt. Mater. **31**, 1061 (2009).
[6] T. R. Schibli, I. Hartl, D. C. Yost, M. Martin, A. Marcinkevičius, M. E. Fermann and J. Ye, Nat. Photon. **2**, 355 (2008).
[7] A. A. Krylov, D. S. Chernykh and E. D. Obraztsova, Opt. Lett. **42**, 2439 (2017).
[8] F. Wang, A. G. Rozhin, V. Scardaci, Z. Sun, F. Hennrich, I. H. White, W. I. Milne and A. C. Ferrari, Nat. Nanotechnol. **3**, 738 (2008).
[9] J. M. Dudley, C. Finot, D. J. Richardson and G. Millot, Nat. Phys. **3**, 597 (2008).
[10] H. Gereon, C. Yao and E. Endl, Med. Laser Appl. **20**,135 (2005).
[11] Z.Y. Yan, X.H. Li, Y.L. Tang, P.P. Shum, X. Yu, Y. Zhang and Q.J. Wang, Opt. Exp. **23**, 4369 (2015).
[12] C. Mou, S. Sergeyev, A. Rozhin and S. Turistyn, Opt. Lett. **36**, 3831 (2011).
[13] Y. Mashiko, E. Fujita and M. Tokurakawa, Opt. Express **24**, 26515 (2016).
[14] P. Hu, Y. Liu, L. Guo, X. Ge, X. Liu, L. Yu and Q. Liu, Appl. Opt. **58**, 7845 (2019).
[15] H. Zhang, D. Y. Tang, R. J. Knize, L. Zhao, Q. Bao and K. P. Loh, Appl. Phys. Lett. **96**, 111 (2010).
[16] W. Pan, J. Zhou, L. Zhang and Y. Feng, J. Light. Technol. **37**, 1333 (2019).
[17] P. Honzatko, Y. Baravets and F. Todorov, Laser Phys. Lett. **10**, 075103 (2013).
[18] H. Liu, A. Luo, F. Wang, R. Tang, M. Liu, Z. Luo. W. Xu, C. Zhao and H. Zhang, Opt. Lett. **39**, 4591 (2014).
[19] P. Yan, A. Liu, Y. Chen, H. Chen, S. Ruan, C. Guo, S. Chen, I. Li, H. Yang and J. Hu, Opt. Mater. Express **5**, 479 (2015).
[20] Y. Chen, G. Jiang, S. Chen, Z. Guo, X. Yu, C. Zhao, H. Zhang, Q. Bao, S. Wen, D. Tang and D. Fan, Opt. Express **23**, 12823 (2015).
[21] Y. Song, S. Chen, Q. Zhang, L. Li, L. Zhao, H. Zhang and D. Tang, Opt. Express **24**, 25933 (2016).
[22] Z. Wang, D. Wang, F. Yang, L. Li, C. Zhao, B. Xu, S. Jin, S. Cao and Z. Fang, J. Light. Technol. **35**, 5280 (2017).
[23] J. Zhu, W. Tian, Z. Gao and Z. Wei, Chin. J. Lasers **44**, 090001 (2017).